한국방재학회논문집
제4권 4호 2004년 12월
pp. 43 ~ 54

수신함수에 의한 한국 지진관측소(인천, 원주 포항) 하부의 지각구조 연구

Crustal Structure Beneath Korea Seismic Stations (Inchon, Wonju and Pohang) Using Receiver function

김 소 구* / 이 승 규**
Kim, So Gu / Lee, Seung Kyu

Abstract

The broadband receiver functions are developed from teleseismic P waveforms recorded at Wonju(KSRS), Inchon(IRIS), and Pohang(PHN), and are analyzed to examine the crustal structure beneath these stations. The teleseismic receiver functions are inverted in the time domain of the vertical P wave velocity structures beneath the stations. Clear P-to-S converted phases from the Moho interface are observed in teleseismic seismograms recorded at these stations. The crustal velocity structures beneath the stations are estimated by using the receiver function inversion method(Ammon et al., 1990). The general features of inversion results are as follows: (1) For the Inchon station, the Conrad discontinuity exists at 17.5 Km(SW) deep and the Moho discontinuity exists at 29.5 Km(NW) and 30.5 Km(SE, SW) deep. (2) The shallow crustal structure beneath Wonju station may be covered with a sedimentary rock of a 3 Km thickness. The average Moho depth is assumed about 33.0 Km, and the Conrad discontinuity may exist at 17.0 Km(NE) and 21.0 Km(NW) deep. (3) For Pohang station, the thickness of shallow sedimentary layer is a 3.0 Km in the direction of NE and NW. The Moho depth is 28.0 Km in the direction of the NE and NW. The Conrad discontinuity can be estimated to be existed at 21.0 Km deep for the NE and NW directions.

key words : broadband receiver function, Ps conversion, Moho discontinuity

요 지

광역 수신 함수가 원주, 인천, 포항 관측소에서 원격 지진 P파로 개발된다. 그리고, 이들 관측소 하부의 지각 구조 해석을 위해서 분석된다. 원격 수신 함수는 관측소 하부 P 파 속도 구조를 위한 시간 영역에서 역산된다. 모호 불연속면에서 P파에서 전환된 S 파가 이들 관측소에서 관측되었다. 관측소의 지하 지각구조는 수신함수 역산으로 산출된다. 1) 인천 관측소에서 Conrad 불연속면은 남서방향에서 17.5Km이고, Moho 불연속면은 북서방향에서 29.5Km와 남동 및 밤서 방향에서 30.5Km이다. 2) 원주 관측소의 경우 천부층의 퇴적층 두께는 3Km인 것으로 해석된다. Moho 깊이는 3.0Km, Conrad 깊이는 북동쪽에서는 17.0Km로, 북서쪽에서는 21.04Km이다. 3) 포항 관측소의 경우, 천부 퇴적암 두께 3Km가 북동 및 북서 방향에서 발견되었다. Moho 깊이는 북동쪽과 북서방향에서 28.04Km인 것으로 해석되며, Conrad 불연속면은 북동과 북서방향에서 21.0Km인 것으로 산출되었다.

Ⅰ. Introduction

The Korean Peninsula, which lies within the margin of the Eurasian plate, has been regarded as a seismically stable land of cratonic nature. Modern seismic activity in the Korean Peninsula is also

* 정회원, 한양대학교 지구해양과학과, 교수 (E-mail: sogukim@hanyang.ac.kr)
** 정회원, 한국지진연구소 선임연구원

relatively low in comparing to that in the neighboring regions including China, Japan, and Taiwan. Up to the present, the deep crustal structure study using seismic waves has not been carried out by means of a seismic method up to date because of the lack of earthquake data in Korea. Crustal structure studies using travel time analysis of some local earthquakes are performed by Kim and Kim (1983), Kim and Lee (1994), and Chung (1995). The investigation by explosive sources was carried out(Kim and Jung, 1985; Kim and Lee, 1996). However it is difficult to find consistency from their crustal models. At present, we can get some broadband teleseismic and deep focus events from INCN station at Inchon, KSRS seismic array at Wonju, and PHN(one of the Pacific Orient Seismic Digital Observation Network(POSEIDON)) station at Pohang(see Fig. 1). So we tried to study the crustal structures using broadband teleseismic and deep focus events of three stations(INCN, KSRS, and PHN) which are located at Wonju(central part), Inchon(central western part), and Pohang (south-eastern part) in the Korean Peninsula.

Considerable interest in the structure of the crust and upper mantle have been generated by the papers of Helmberger and Wiggins (1971), Burdick and Langston (1977), Langston (1977a, 1977b, and 1979), Owens *et al.* (1984, 1987), Liu and Kind (1987), Priestly *et al.* (1988), Owens (1987), Owens and Crosson (1988), Ammon *et al.* (1989, 1990), Ammon (1991), McNamara and Owens (1993), and Zhu *et al.* (1995). Marc (1988) has used deep focus(focal depth $\geq$ 117 Km) events to study a lateral variation of upper mantle structure beneath New Caledonia. The models that have been proposed by these authors show many similarities but differ substantially in detail. It has been shown that the converted phases can be used not only for determining the depth of discontinuities in the earth, but also for investigating their lateral fluctuations. A specific converted phase within the body wave train is associated with a specific interface and its time delay mainly on the depth and structure of the interface underneath the receiver.

The purpose of this study is to determine the vertical P velocity distributions beneath the recording sites(INCN, KSRS, and PHN) by using the receiver function inversion method proposed by Ammon *et al.* (1990).

2. Broadband Teleseismic and Deep Focus Events

We used the broadband 3-component data recorded at the three stations. Fig. 1(upper figure) shows the seismic stations and teleseismic event locations. The INCN station is one of the IRIS(The Incorporated Research Institution for Seismology) global seismic network which is equipped with very broadband three-components STS-1 sensors and recorded with a sampling rate of 20 sps(samples per second). The KSRS seismic arrays are located at Wonju in Korea, which is equipped with broadband seismometer (model KS36000) of 20 sps. The PHN station is one of the POSEIDON(Pacific Orient Seismic Digital Observation Network), which is equipped with broadband sensor and recorded with a sampling rate of 10 sps. All seismograms are broadband velocity recordings. For the Pohang station, we tried to find some deep focus(depth$\geq$ 440Km) like KSRS and teleseismic events to avoid multiple phases in the source time function(Marc, 1988). Fig. 1(lower figure) shows the clusters of the teleseismic data for stations INCN, KSRS and PHN. The detailed parameters of the earthquakes are listed in Table 1. Theoretical backazimuth and incidence angle of the receiver area are calculated by using EDABAC(II) software(Herrmann,1994).

The teleseismic P waveforms contain information about near-source and near-receiver structure. Using the method of Langston (1979), the source and distance path effects can be removed from P waveforms by deconvolving the vertical from the horizontal components. The source-path equalized waveform is called the receiver function and is most sensitive to the P-to-S conversion from structures beneath the recording sites(Owens *et al.*, 1984), The radial receiver functions are often modeled by horizontally stratified velocity structure using time-domain inversion technique(Owens *et al.*, 1984; Ammon *et al.*, 1990). This method has been applied

to numerous areas and is efficient in estimating the velocity-depth variation of the crust. Receiver functions are extracted from the three-components broadband recordings of teleseismic and deep focus(only used for the PHN station) P waveforms. The receiver functions obtained by deconvolving method (Langston, 1979) are assumed to be free of source, mantle-path, and instrument response effects. The deconvolution is performed in the frequency domain(Ammon, 1991) using a Gaussian filter width of 4.0(INCN and KSRS stations) and 2.5(PHN station) and water-level (trough filler) of 0.001(INCN and KSRS) and 0.01(PHN station) according to S/N ratio and sampling rate, which produced stable deconvolution. True amplitudes of receiver functions are preserved in the deconvolution process. The use of true amplitudes preserves information about the shallow velocity structure (Ammon, 1991). The receiver functions have been extracted from many events clustered in distance and backazimuth ranges. These receiver functions are stacked to enhance signal-to-noise ratio.

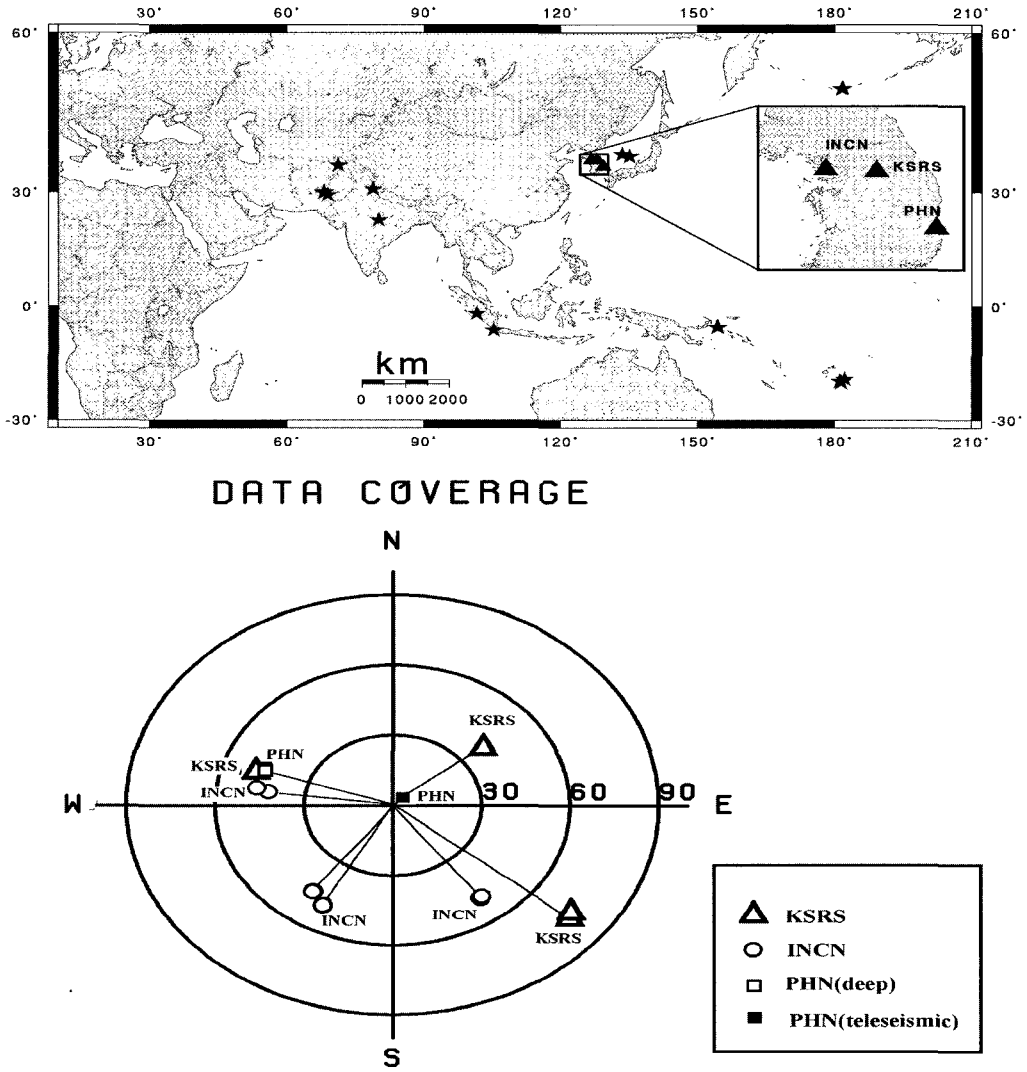

Fig. 1. (upper) Map showing three stations(closed triangles) and teleseismic and deep focus events(closed asterisks). INCN(IRIS station at Incheon), KSRS(at Wonju), and PHN (POSEIDON station at Pohang) and (lower)teleseismic data coverage at Incheon, Wonju, and Pohang stations. The size of symbol indicates a difference of event magnitudes. Events used in stacked receiver functions are listed in Table 1. The numbers are epicentral distances in degree.

Table 1. Seismic parameters for teleseismic and deep focus events for receiver function analysis

Stations		O.T.(UT)		Distance	BAZ	Epicenter		Depth	Mag.
		m/d/yr	h:m:s	(deg)	(deg)	Lat.	Lon.	(Km)	(mb)
INCN	SE	8/16/95A	10:27:28.60	50.10	143.20	-5.80	154.17	30.0	6.5
		8/16/95B	23:10:23.90	50.20	143.00	-5.77	154.34	33.0	6.2
	SW	10/ 6/95	18: 9:45.90	45.80	216.40	-2.09	101.41	33.0	5.8
		3/17/95	8: 5:48.50	48.20	209.10	-6.62	105.19	33.0	6.0
	NW	2/27/97A	21: 8: 2.40	48.60	279.20	29.90	68.10	6.0	6.5
		2/27/97B	21:30:36.60	48.70	279.40	30.01	67.98	33.0	6.1
		3/ 4/97	13: 3:47.00	48.30	278.20	29.36	68.82	33.0	5.9
KSRS	NE	8/19/96	4:19:15.60	39.90	51.90	51.43	-178.45	33.0	5.7
		8/31/96	20:47:23.00	40.00	51.90	51.41	-178.23	33.0	5.8
	SE	7/20/96B	7:41:15.40	76.50	128.10	-19.77	-177.77	365.0	5.7
		8/ 5/96	22:38:22.10	76.70	129.20	-20.61	-178.54	530.0	6.5
		10/19/96	14:53:48.00	76.20	129.30	-20.29	-178.86	590.0	6.0
	NW	2/27/97A	21: 8: 2.40	49.60	279.80	29.90	68.10	6.0	6.5
		2/27/97B	21:30:36.60	49.70	280.00	30.01	67.98	33.0	6.1
PHN	NE (deep.)	1/19/93	14:39:26.10	4.20	50.10	38.65	133.46	448.0	6.0
		3/31/95	14: 1:40.00	5.00	62.60	38.21	135.01	354.0	6.0
	NW (tele.)	7/14/91	9: 9:11.90	46.40	288.50	36.33	71.11	212.0	6.4
		10/19/91	21:23:14.30	42.20	277.90	30.78	78.77	10.0	6.5

※ BAZ(backazimuth) are calculated by using EDABAC(II) software(Herrmann,1994).

Fig. 2 shows individual and stack radial receiver functions for INCN(a), KSRS(b), and PHN(c) stations. Ray parameter p(sec/Km) are indicated in Fig. 2. All are plotted in the same scale. The Moho Ps phases approximately 3.7 ~ 4.0 seconds after the direct P arrival are shown for INCN and KSRS stations. Two or three small converted Ps phases between the direct P and the Moho Ps arrivals indicate to exist many discontinuities within the crust. Especially for the PHN station, we know that the direct P phase lag(0.4 ~ 0.5sec) for the radial receiver functions appeared. A shallow basin(< 5Km deep) introduces a phase lag in the first(0sec) pulse in receiver functions, by interference between direct P and phase conversions at the bottom of the basin(Sheehan et al., 1995). The phase delays are seen for all records from the PHN station. We model the radial receiver functions from the NW, SW, and SE backazimuths for INCN station assuming isotropic and plane-layered crustal structure. For KSRS station, we model the radial receiver functions from NW, SE, and NE backazimuths. For PHN station, the radial receiver functions are modeled from NW (teleseismic events) and NE(deep focus events) backazimuths.

3. A *Priori* Models at Stations INCN, KSRS, and PHN

At first, we chose a priori model for each station using the forward modeling technique proposed by Langston (1977b). Fig. 3 shows the five models from the previous studies in the Korean Peninsula. The five velocity models are not well consistent in P-wave velocities and depths of the Moho discontinuity. So we tested to fit the stack receiver functions with the synthetics from the five models. For the forward modeling, we used ray parameter p=0.075sec/Km, water-level=0.001, and Gaussian filter width=4.0 to generate the synthetic radial receiver functions. Fig. 4 shows the synthetic radial receiver functions for the five models. We can selected two models(Model B and C) which are well fitting with the Moho Ps phase arrival. We have also tried to find more closed models for three stations by using the selected two models. To determine the simple initial model, we have compared observed relative arrival times for corresponding phases with computed ones for previous velocity models. We determined three initial simple velocity models which consist of a 4 or 5 layered structure from forward model tests.

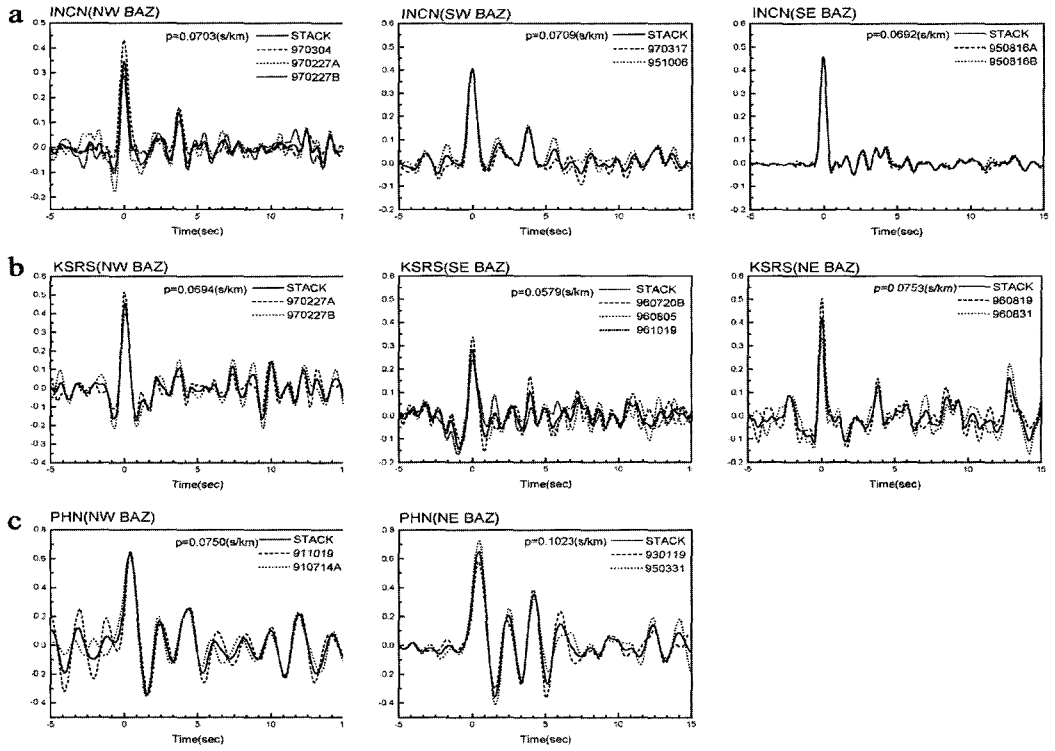

Fig. 2. Stacked and individual radial receiver functions for three backazimuths from station INCN(a), KSRS(b), and PHN(c). Ray parameter p and events in computing each stack are indicated. All are plotted in the same scale.

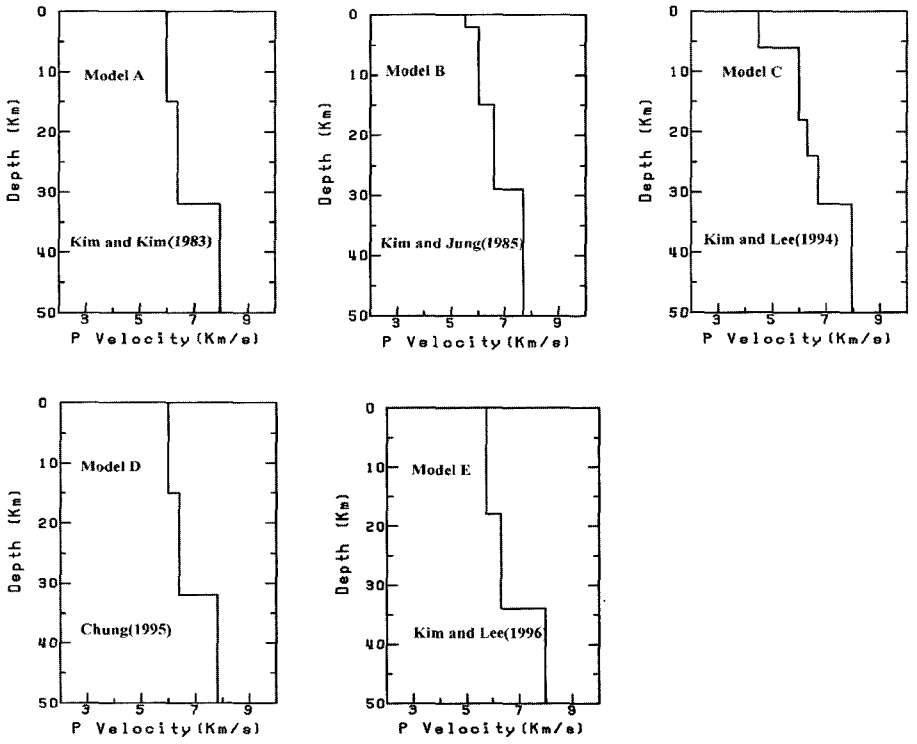

Fig. 3. Velocity models in the Korean Peninsula are shown which are from previous studies. The inserted letters of five models indicate the authors of previous studies.

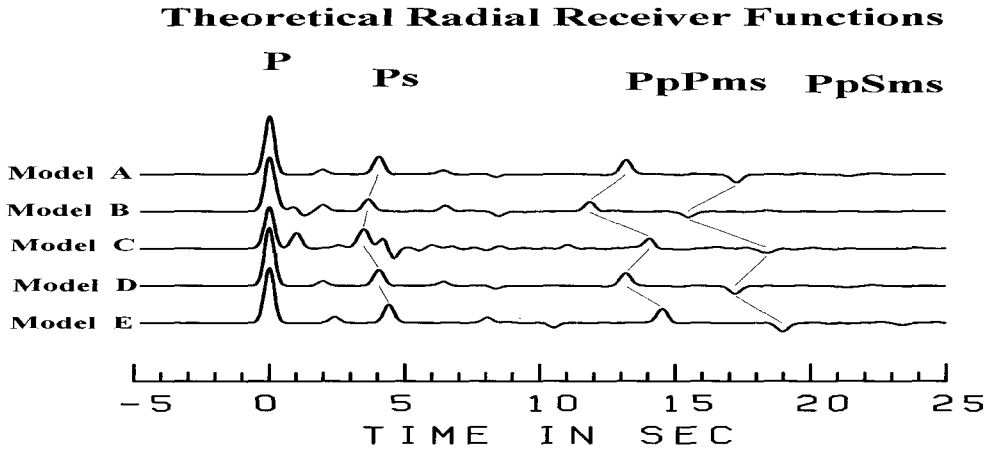

Fig. 4. The synthetic radial receiver functions using five models of Figure 3. Among the models, Model B and C are well fitted with a Ps-P arrival time of observed radial receiver functions.

At last, we have selected three initial velocity models for three stations in order to invert receiver functions(see Fig. 5). For the INCN and KSRS stations, we have taken the modified velocity model from Model B, C in Fig. 3 which are well fitted with the observed stack radial receiver functions. For PHN station, the initial model is made with a low velocity layer at 8 Km deep. These three models are used for inversions as the initial model for stations INCN, KSR, and PHN.

4. Receiver Function Inversion Models

The stacked receiver functions were inverted using the linearized time domain waveform inversion method proposed by Ammon *et al.* (1990) of which algorithms are improved with the modified fast partial derivatives of Randall (1989) and included a smoothness constraint on all the resulting velocity models utilizing the "Jumping" inversion technique of Shaw and Orcutt (1985). The receiver function inversion scheme of Ammon *et al.* (1990) consists of a linearized-iterative, least-squares waveform fitting. The algorithm has a merit in which computational efficiency coupled with an implementation of smoothness constraint allows more flexible models and the methods are applied to minimize the energy in the second difference of the model parameters. To compute modeled receiver functions for a given velocity structure, a technique based on propagator matrix method is used(Kennett ,1983).

In this study, we assumed $V_p = \sqrt{3}\, V_s$ and density $\rho = 0.32\, V_P + 0.77$ (Berteussen, 1977), where ρ(g/㎤) represents density, V_P and V_s(Km/sec) represent P- and S-wave velocity assuming a Poisson's ratio of 0.25. We used a small amount of a smoothness during inversions(smoothness parameter σ= 0.1 to 0.3). The earth structure is parameterized by a series of plane horizontal layers which parameterized a 0.5 Km thickness layer for shallow structures(1.0 or 2.0Km deep), a 1.0 Km thickness layer from 2 Km to 7 Km deep, and 2~4 Km thickness layer below the depth of 7 Km for the three stations. We generate 36 different initial models from each initial model by perturbing them with a cubic perturbation of 1.0Km/sec and 20% random component(Ammon *et al.*, 1991). The inversions quickly converge within five iterations. We repeat inversions for each perturbed initial model to find reasonable velocity model for the three stations. The iterative procedure is used to minimize the residuals between the observed radial receiver functions and the synthetic model by a modelled structure. Our Moho picks are based on the nature of crust-mantle transition, i.e., the first increase in velocity either sharply or with a gradient at expected velocity for the Moho.

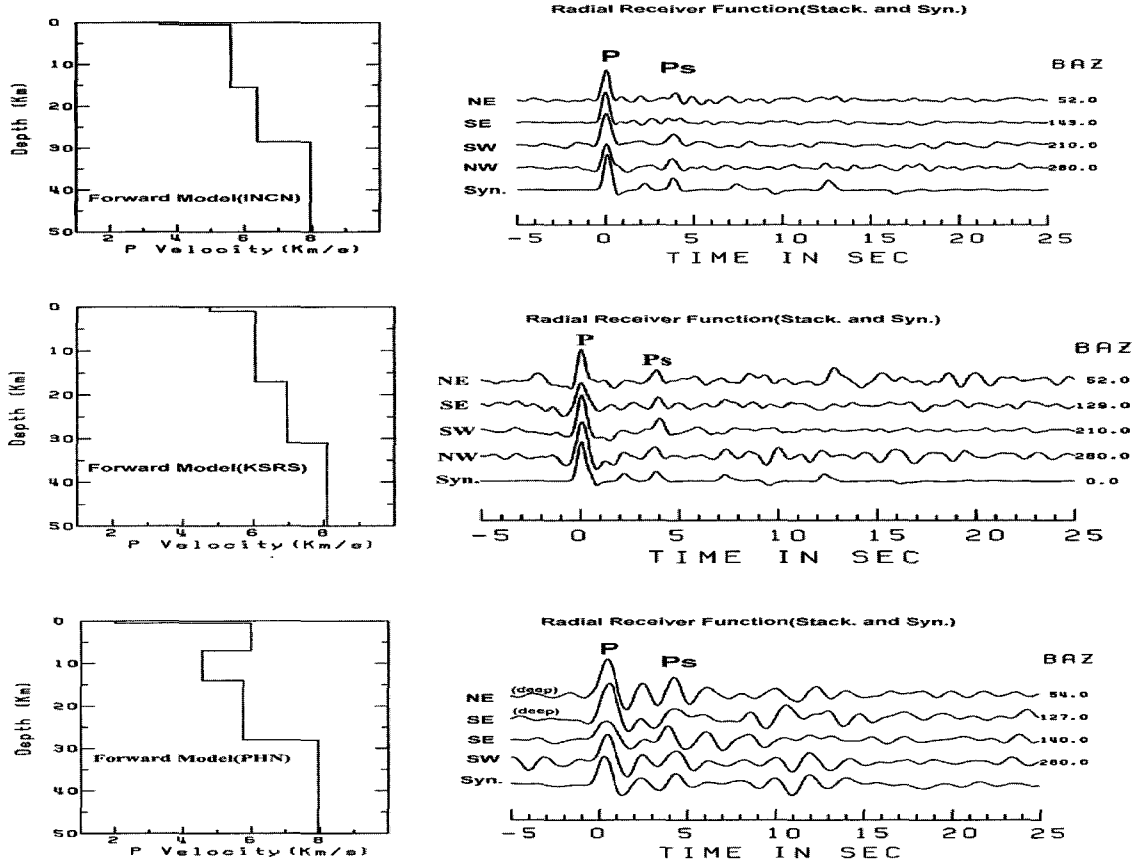

Fig. 5. (left) Velocity models from the forward modeling are indicated for stations INCN, KSRS, and PHN from the top. Right figures indicate stack radial receiver functions and theoretical receiver function calculated by using the left velocity models.

1) The INCN station

Fig. 6 shows final velocity models(SE, SW, and NW backazimuths) for INCN station. The stack radial receiver functions of SE backazimuth can show weak Ps phases. The Ps phases may indicate that there is at least three discontinuities in the crust. It is also difficult to discriminate the Moho Ps phase because of weakness and unclearing. Fig. 6a shows the final velocity model of SE direction of which velocity model shows constant velocity from the top to 9.5 Km deep and a gradient at 25~33 Km deep. In this model, we can assume that the Moho depth is 29.5 Km to infer the Ps-P time of 3.8 sec. The main features of the velocity model of SW direction are a velocity increase in the upper 4.5 Km, a discontinuity at 12.5 Km deep, and a crust-mantle transition between depths of 28.0 and 30.5 Km in Fig. 6b. The Moho Ps phase of radial receiver function in the direction of NW is clear and strong as much as one of SW direction. The velocity model of NW direction indicates a upper crust of 4.5 Km thickness and a crustal thickness of 29.5 Km (see Fig. 6c).

2) The KSRS station

Fig. 7 shows the final velocity models(NE, SE, and NW backazimuths) for KSRS station. Fig. 7a shows the final velocity model of NE direction of which discontinuities can be seen a 2.5 Km deep, a nearly constant velocity from 7.5 to 31 Km deep, and a gradient at 31~35 Km deep. In this model, the Moho depth is assumed to 33.0 Km. The main features of the velocity model of SE direction are a velocity increase in the upper 3.5 Km, a discontinuity at 17 Km deep, and a crust-mantle transition between depths of 30.5 and 35 Km in Fig. 7b. The velocity model of NW direction can be seen

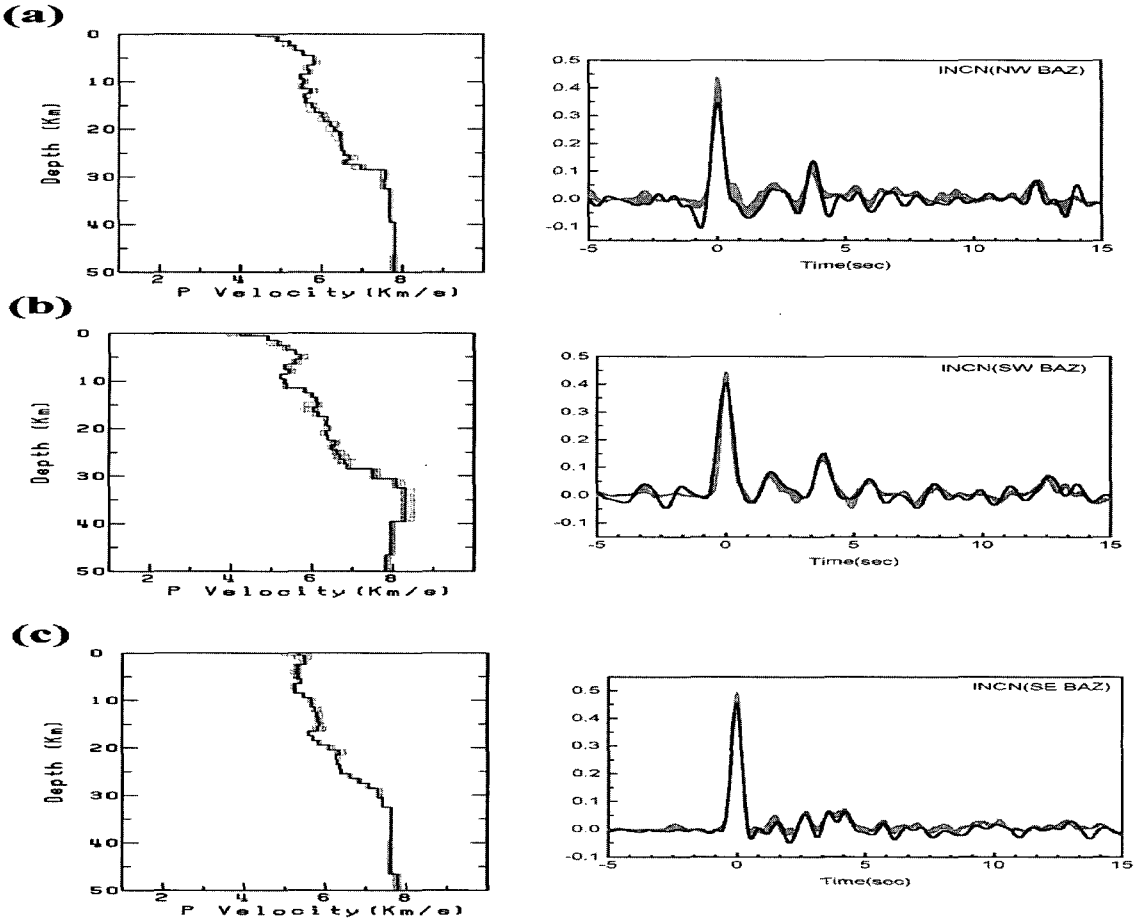

Fig. 6. Inversion results of station INCN in the directions of NW(a), SW(b), and SE(c) backazimuths from the top. Final(thick solid) P wave velocity model takes the mean of acceptable inversion models(thin dashed) from many inversion models. (left) Receiver function waveform fit. Thick solid line indicates a stacked radial receiver function and the shaded region represents the synthetic radial receiver functions from acceptable inversion velocity models.

a upper crust of 3.0 Km thickness, a low velocity zone(5.8~6.2 Km/sec) from 7 to 18 Km deep, and a crustal thickness of 33.0 Km(see Fig. 7c).

3) The PHN station

Fig. 8 shows the final velocity models for NE and NW directions under the Pohang station. The velocity model of the NE(deep focus) indicates a sedimentary layer of 3.0 Km thickness, a high velocity layers at 3 Km and 7 Km deep, a low velocity zone at 10 Km deep, a discontinuity at 21 Km deep, and the Moho discontinuity at 28 Km deep(see Fig. 8a). For teleseismic events in the direction of 280° backazimuth, there is a sedimentary layer of 3 Km thickness from the top, a high velocity layer at 3~9 Km deep, a discontinuity at 21 Km deep, and the Moho discontinuity(Vp=7.9 Km/sec) at 28 Km deep in Fig. 8b. We notice that the phase lag in the zero phase in receiver functions is due to a shallow basin as shown in the studies of the Colorado Rocky Mountain(Sheehan et al.,1995). The geology of the Pohang(PHN station) area consists of volcanic and sedimentary rocks, mostly younger than the Cretaceous. It is possible that deposits of thick sedimentary rocks occurred in the Pohang area during the Quaternary deposits which are the Alluvium and the Marine terraces(Lee and Kim, 1990).

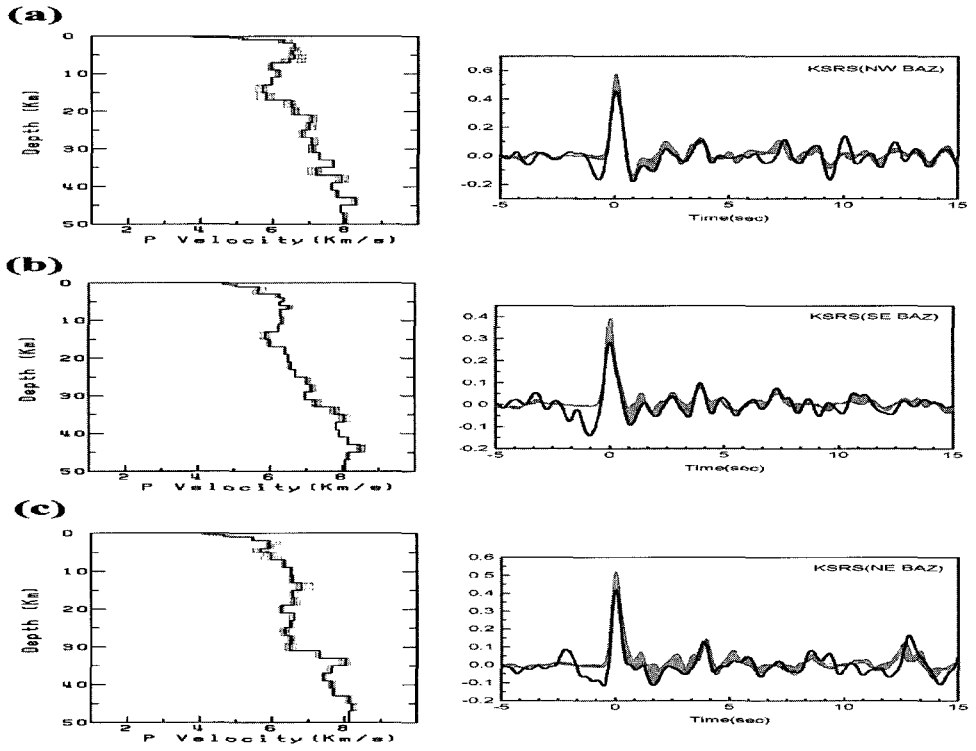

Fig. 7. Inversion results of station KSRS in the directions of NW(a), SE(b), and NE(c) backazimuths from the top. Final(thick solid) P wave velocity model takes the mean of acceptable inversion models(thin dashed) from many inversion models. (left) Receiver function waveform fit. Thick solid line indicates a stacked radial receiver function and the shaded region represents the synthetic radial receiver functions from acceptable inversion velocity models.

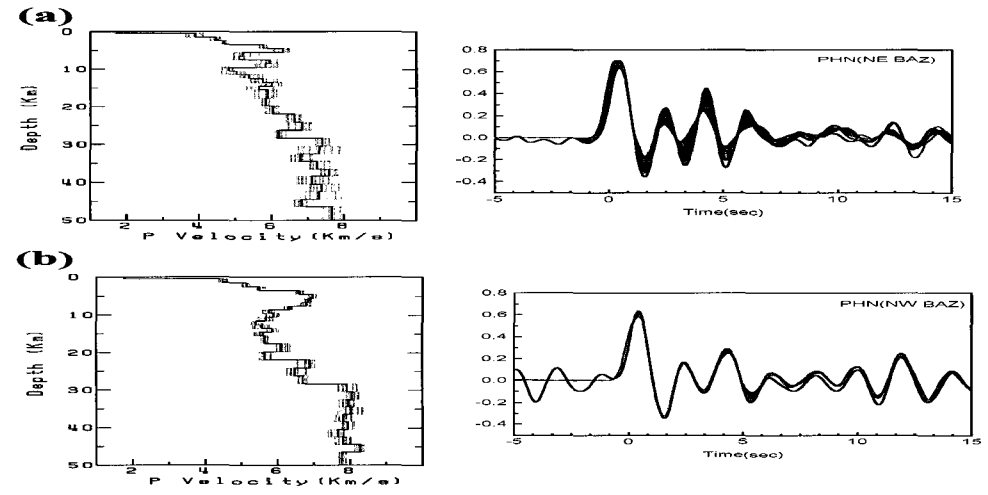

Fig. 8. Inversion results of station PHN in the directions of NE(a) and NW(b) backazimuths from the top. Final(thick solid) P wave velocity model takes the mean of acceptable inversion models(thin dashed) from many inversion models. (left) Receiver function waveform fit. Thick solid line indicates a stacked radial receiver function and the shaded region represents the synthetic radial receiver functions from acceptable inversion velocity models. For the station PHN, P phase lag of 0.4 sec can be observed from all records. The direct P lags indicate the sediment effect of a shallow basin(Sheehan et al., 1995).

5. Result and Discussion

The stations INCN and KSRS are located in the central part of the Korean Peninsula, and the PHN station is located in the southeastern part of the Korean peninsula. The geological structure of the PHN station is different from the other stations. The seismotectonics of the Pohang (PHN) area are the Cenozoic depression and graben(Kim and Gao, 1995) within the Kyongsang Sedimentary Basin. On the other hand, the seismotectonics of Inchon(INCN) and Wonju(KSRS) station include of the Kyonggi massif, platforms of which the strike is N50°E (Lee and Kim, 1990).

From inversion results, we can estimate that the Moho discontinuity exists at a 30.5 Km deep for the INCN station and at 33.0 Km deep for the KSRS station, and at 28.0 Km deep for the PHN station, respectively. The model of the INCN station is consistent the results from Kim and Kim (1983), Kim and Lee (1994), and Chung (1995) for the Moho depth. For the KSRS station, the depth of the Moho discontinuity is consistent with Kim and Lee (1996). The model of the PHN station is consistent with the result from Kim and Jung (1995). The P velocities increase from 1.8 Km/sec at surface to 5.4 Km/sec at 3 Km depth which consists of sediments and sedimentary rock. The inversion results from the teleseismic events for NW backazimuth at the shallow velocity structure(< 4 Km) are the same as the result using deep focus events. All of the first P arrivals are at the Pohang station are delayed 0.4 sec, and the direct P lags indicate the sediment effects of a shallow basin(Sheenhan *et al.*, 1995). The upper crust high velocity zone at 4~5 Km deep and the middle crust low velocity zone at 10 Km deep are found in the directions of NE and NW backazimuths at station PHN which coincides with a study on the regional high gravity anomaly of +50~+60mgal, whereas the Kyongsang basin has low gravity anomaly of +20 mgal(Cho *et al.*, 1996). Li (1997) also determined the Moho depth as 29.5 Km at the Pohang basin by means of 3-D seismic tomography. He also demonstrated the high P-wave velocity at about 4 Km and the low velocity layer at 10 Km in his study. This is very agreeable with our results from the receiver functions. The waveform fit residuals for each station are taken with less than 4% for rms errors in this study like previous ones(Kim and Lee, 1996).

6. Acknowledgment

This study was supported by Hanyang University and Korea Meteorological Admini stration(KMA).

REFERENCES

Ammon, C. J., J. Zucca, and P. Kasameyer, An S-to-P converted phase recorded near Long Valley/Moho Craters Region, California, *J. Geophys. Res.*, 94(B12), 17721-17727, 1989.

Ammon, C., G. Randall, and G. Zandt, On the nonuniqueness of receiver function inversions, *J. Geophys. Res.*, 95(B10), 15303-15318, 1990.

Ammon, C. J., The isolation of receiver effects from telesiemic P waveforms, *Bull. Seism. Soc. Am.*, 81(6), 2504-2510, 1991.

Berteussen, K. A., Moho depth determinations based on spectral ratio analysis of NORSAR long-period P waves, *Phys. Earth Planet. Inter.*,31, 313-326, 1977.

Burdick, L. J. and C. A. Langston, Modeling crustal structure through the use of converted phases in teleseismic body -wave forms, *Bull. Seism. Soc. Am.*, 67(3), 677-691, 1977.

Cho J.D., J.H. Choi, M.T. Lim, I.H. Park, and I. S. Ko, A study on the regional gravity anomaly (southern part of Korean Peninsula), *KIGAM Research Report (KR-96(c)-5)*, 27p (in Korean), 1996.

Chung T. W., A quantitative study on the crustal structure of the Korean Peninsula, *Jour. Korean Earth Society* , 16, 152-157, 1995.

Haskell, N. A., Crustal reflection plane P and SV waves, *J. Geophys. Res.*, 67, 4751 -4767, 1962.

Helmberger, D. and R. A. Wiggins, Upper mantle structure of midwestern United States, *J. Geophys. Res.*, 76 (14), 3229 -3245, 1971.

Herrmann, R. B., Computer Programs in Seismology, Saint Louis University, 1994

Kennett, B. L. N., Seismic Wave Propagation in

Stratified Media, Cambridge University Press, New York, 342, 1983.

Kim Sang Jo and So Gu Kim, A study on the crustal structure of south Korea by using seismic waves, *J. Korean Inst. Mining Geol.*, 16,51-61(in Korean), 1983.

Kim So Gu and Seoung Kyu Lee, Crustal modelling for the southern parts of the Korean Peninsula using observational data and ray method, *Kor. Inst. Min. and Energ. Res.*, 31, 549-558(in Korean), 1994.

Kim So Gu and Fuchun Gao, *Korean Earthquake Catalogue*, The Seismological Institute of Hanyang University, 98p., 1995.

Kim So Gu and Seoung Kyu Lee, Seismic velocity structure in the Central Korean Peninsula using the artificial explosions, *Bull. Seis. Assoc. Far East*, SAFE 2(1), 4-17, 1996.

Kim S. K. and B. H. Jung, Crustal structure of the southern part of Korea, *J. KoreanMining Geol.*, 18. 151 - 157 (in Korean), 1985.

Langston, C. A., Corvallis, Oregon, crustal and upper mantle receiver structure from teleseismic P and S waves, *Bull. Seism. Soc. Am.*, 67, 713-724, 1977a.

Langston, C. A., The effect of planar dipping structure on source and receiver responses for constant ray parameter, *Bull. Seism. Soc. Am.*, 67, 1029-1050, 1977b.

Langston, C. A., Structure under Mount Rainier, Washington, inferred from teleseismic body waves, *J. Geophys. Res.*, 84(B9), 4749-4762, 1979.

Lee, D.Y. and J.Y. Kim, Quaternary Geology of the Pohang-Youngil Area, *KIER-Research Report* (KR-90-1A-2)(in Korean), 1990.

Li, Qinghe, 3-D crustal velocity tomography in the southern part of South Korea, personal communication (unpublished technical report), 1997.

Liu, Qiyuan and R. Kind, Lateral variations of the structure of the crustal-mantle boundary from conversions of teleseismic P *waves, J. Geophysics,* 60, 149-156, 1986.

Marc, R., Lateral Variation of Upper Mantle structure beneath New Caledonia determined from P-wave receiver function: evidence for a fossil subduction zone. *Geophysical J. Int.*, 95,561-577, 1988.

McNamara, D. E. and T. J. Owens, Azimuthal shear wave velocity anisotropy in the basin and range province using moho Ps converted phases, *J. Geophys. Res.*, 98 (B7), 12003-12017, 1993.

Owens, T. J., G. Zandt and S. R. Taylor, Seismic evidence for an ancient rift beneath the Cumberland Plateau, Tennessee: A detailed analysis of broadband teleseismic P waveforms, *J. Geophys. Res.*, 89(B9), 7783-7795, 1984.

Owens, T. J., S. R. Taylor, and G. Zandt, Crustal structure at regional seismic test network stations determined from inversion of broadband teleseismic P waveforms, *Bull. Seism. Soc. Am.*, 77(2), 631-662, 1987.

Owens, T. J., Crustal structure of the Adirondacks determined from broadband teleseismic waveform modeling, *J. Geophys. Res.*, 92(B7), 6391-6401, 1987.

Owens, T. J. and R. S. Crosson, Shallow structure effects on broadband teleseismic P waveforms, *Bull. Seism. Soc. Am.*, 78(1), 96-108, 1988.

Özalaybey, S. , M.K. Savage, A.F. Sheehan, J.N. Louie, and J.N. Brune, Shear -Wave Velocity Structure in the Northern Basin and Range Province from the Combined Analysis of Receiver Functions and Surface Waves, *Bull. Seism. Soc. Am.*, 87(1), 183- 199, 1997.

Peng, X. and E. D. Humphreys, Moho Dip Crustal Anisotropy in Northwestern Nevada from Teleseismic Receiver Functions, *Bull. Seism. Soc. Am.*, 87(3), 745-754, 1997.

Priestly, K. F., G. Zandt, and G. E. Randall, Crustal structure in Eastern Kazakh, U.S.S.R. from teleseismic receiver functions, *Geophys. Res. Lett.*, 15(6), 613 -616, 1988.

Randall, G. E., Efficient calculation of differential seismograms for lithospheric receiver functions, *Geophysical J. Int.*, 99, 469-481, 1989.

Shaw, P. R., and J. A. Orcutt, Waveform inversion of seismic refraction data and applications to young Pacific crust, *Geophys. J. R. Astron.* Soc., 82, 375-414, 1985.

Sheehan, A.F., G.A. Abers, C.H. Jones, and A.L.

Lerner-Lam, Crustal thickness variations across the Colorado Rocky Mountain from teleseismic receiver functions, *J. Geophys. Res.*, 100(B10), 20391-20404, 1995.

Zhang, J. and C. A. Langston, Dipping Structure under Dourbes, Belgium, Determined by Receiver Function Modeling and Inversion, *Bull. Seism. Soc. Am.*, 85, 254-268, 1995.

Zhu, L., T. J. Owens, and G. E. Randall, Lateral variation in crustal structure of the northern Tibetan Plateau inferred from teleseismic receiver functions, *Bull. Seism. Soc. Am.*, 85(6), 1531-1540, 1995.

◎ 논문접수일 : 2004년 11월 22일
◎ 심사의뢰일 : 2004년 11월 24일
◎ 심사완료일 : 2004년 12월 25일